Universal fluctuations and squeezing in a generalized Dicke model near the superradiant phase transition

D. S. Shapiro,[1,2,3,*] W. V. Pogosov,[1,4] and Yu. E. Lozovik[1,5,6]

[1]*Dukhov Research Institute of Automatics (VNIIA), 127055 Moscow, Russia*

[2]*Department of Physics, National Research University Higher School of Economics, 101000 Moscow, Russia*

[3]*Laboratory of Superconducting Metamaterials, National University of Science and Technology MISiS, 119049 Moscow, Russia*

[4]*Institute for Theoretical and Applied Electrodynamics, Russian Academy of Sciences, 125412 Moscow, Russia*

[5]*Institute of Spectroscopy, Russian Academy of Sciences, 142190 Moscow Region, Troitsk, Russia*

[6]*Moscow Institute of Physics and Technology, Dolgoprudny, Moscow Region 141700, Russia*

(Received 21 September 2019; revised 9 June 2020; accepted 9 July 2020; published 7 August 2020)

In view of recent proposals for the realization of anisotropic light-matter interaction in such platforms as (i) nonstationary or inductively and capacitively coupled superconducting qubits, (ii) atoms in crossed fields, and (iii) semiconductor heterostructures with spin-orbital interaction, the concept of a generalized Dicke model, where coupling strengths of rotating wave and counter-rotating wave terms are unequal, has attracted great interest. For this model we study photon fluctuations in the critical region of normal-to-superradiant phase transition when both the temperatures and numbers of two-level systems are finite. In this case, the superradiant quantum phase transition is changed to a fluctuational region in the phase diagram that reveals two types of critical behaviors. These are regimes of Dicke model (with discrete $\mathbb{Z}_2$ symmetry), and that of anti-Tavis-Cummings and Tavis-Cummings $U(1)$ models. We show that squeezing parameters of photon condensate in these regimes show distinct temperature scalings. Besides, relative fluctuations of a photon number take universal values. We also find a temperature scale below which one approaches a zero-temperature quantum phase transition where quantum fluctuations dominate. Our effective theory is provided by a non-Goldstone functional for condensate mode and by Majorana representation of Pauli operators. We also discuss the Bethe ansatz solution for integrable $U(1)$ limits.

DOI: 10.1103/PhysRevA.102.023703

I. INTRODUCTION

An important concept of contemporary quantum optics and cavity quantum electrodynamics is a single mode version of a Dicke model [1], where an ensemble of two-level systems interacts with a quantized electromagnetic field in a cavity, microwave resonator, etc. This model demonstrates superradiant phase transition, a collective phenomenon characterized by condensation of a macroscopic number of photons. Experimental signatures of second-order quantum phase transition, equivalent to the superradiant one, were observed in a driven Bose-Einstein condensate of Rb atoms in an optical cavity [2]. Also, the engineering of the Dicke model simulator with cold Be atoms in an optical trap and signatures of superradiant phase transition were reported in [3]. The physics of the Dicke model is believed to be tested in quantum metamaterials such as superconducting qubits arrays [4–7] integrated with a GHz transmission line via tunable couplers [8–11]. The recent advances in implementations of strong coupling regimes in superconducting circuits [12–15] are promising for realizations of phase transitions as well. Extremely fast emission, indicating a superradiant pulse, was observed in a lumped resonator coupled to an inhomogeneously broadened macroscopic ensemble of nitrogen-vacancy centers [16,17].

Thank to advances in fabrication technologies of light-matter hybrid systems during the last few years, an interest in generalizations of the Dicke model has emerged. The behavior in the presence of incoherent pumping or cavity loss reveals a richness of phase diagrams, see Ref. [18] for a review. In the present work we are focused on another example of generalization, the anisotropic qubit-cavity interaction, i.e., when strengths of rotating- and counter-rotating-wave terms are different. The possible physical realizations are frequency modulated [19] or inductively and capacitively coupled [20] superconducting qubits, semiconductor heterostructures with spin-orbital interaction [21], and atoms in crossed electric and magnetic fields, see Ref. [22] for a review and also references therein.

The Hamiltonian of the generalized Dicke model (GDM) reads as

$$\hat{H} = \omega \hat{a}^\dagger \hat{a} + \frac{\epsilon}{2}\hat{S}_z + \frac{g}{\sqrt{N}}(\hat{a}\hat{S}^+ + \hat{a}^\dagger \hat{S}^-) + \frac{J}{\sqrt{N}}(\hat{a}\hat{S}^- + \hat{a}^\dagger \hat{S}^+). \quad (1)$$

The first term describes the single-mode photon field of the excitation frequency ω; here $\hat{a}^\dagger$ and $\hat{a}$ are, respectively, creation and annihilation operators. The second term is the

*shapiro.dima@gmail.com

Hamiltonian of the ensemble consisting of N two-level systems. They have equal energy splittings ϵ between their ground and excited states. The collective angular momentum operator $\hat{S}^z = \sum_{j=1}^{N} \hat{\sigma}_j^z$ is a sum over individual Pauli operators $\hat{\sigma}_j^z$ (each of them acts upon the jth two-level system in the ensemble). The upper/lower operators of a collective "spin" $\hat{S}^{\pm} = \sum_{j=1}^{N} \hat{\sigma}_j^{\pm}$ are also sums over respective $\hat{\sigma}_j^{\pm}$. The light-matter coupling is encoded by the two last terms in (1): the rotating-wave term with the coupling strength g corresponds to the resonant interaction, and the counter-rotating term with J corresponds to the antiresonant one.

A rigorous field-theoretical description of the superradiant phase transition in thermodynamic limit $N \to \infty$ was proposed by Popov and Fedotov [23] in Matsubara formalism. The solution was obtained in the rotating wave approximation (RWA), when antiresonant terms are neglected, i.e., $J = 0$. This case is also known as the Tavis-Cummings model (TCM). The phase transition is of second order, it occurs if the temperature is lower than a critical value $T < T_c$. The coupling constant must be higher than a critical value $g > g_c$, otherwise the system remains in normal phase for any temperature. The critical coupling $g_c = \sqrt{\omega\epsilon}$ does not depend on N due to $1/\sqrt{N}$ normalization in (1); the critical temperature is $T_c = \epsilon(2 \operatorname{arctanh}\frac{g_c^2}{g^2})^{-1}$.

Phase transition in RWA was also studied in alternative situations. They include a regime of fixed excitations density and finite chemical potential [24,25], and zero temperature regime [26] where Bethe ansatz technique was applied. The study of fluctuational normal-to-superradiant transition at finite temperatures and beyond the thermodynamic limit was presented in Ref. [27].

According to a contemporary view on normal-to-superradiant quantum phase transition (QPT) in the symmetric Dicke model with $J = g$, it is characterized by quantum chaotic dynamics [28,29] and dissipationless thermalization [30]. QPT is of second order as in RWA, however, the critical coupling is $g_c/2$. The analysis of scaling behavior near QPT at finite N was provided in Ref. [31]. Recently, an analysis of quantum chaos in the symmetric Dicke model via out-of-time-ordered correlators attracted great interest [32–34].

We also note that the superradiance is not a unique QPT in this model. Another one is known as a classical oscillator limit of $\omega = 0$, where a finite-N phase diagram of a ground state is rather rich showing noncritical and critical entanglement [35].

Generalizations of QPT on the case of $g \neq J$ were studied in Refs. [20,36–38]. A schematic phase diagram in the thermodynamic limit is depicted in Fig. 1. The superradiant phase exists in the domain defined by $g + |J| > g_c$ which determines second-order phase transition. If $g > 0$ and J may change its sign, then $J = 0$ is the line of first-order phase transition between the superradiant phases of "electric" ($J > 0$) and "magnetic" ($J < 0$) types [20]. The criticality and diagram of magnetic and electric phases at finite N were analyzed in Ref. [38].

In contrast to the previous studies of QPT in the generalized model, we study the regime of finite T and N in the present paper. Employing the path integral approach of Ref. [27], we go beyond RWA to an asymmetric light-matter interaction and explore photon condensate fluctuations near

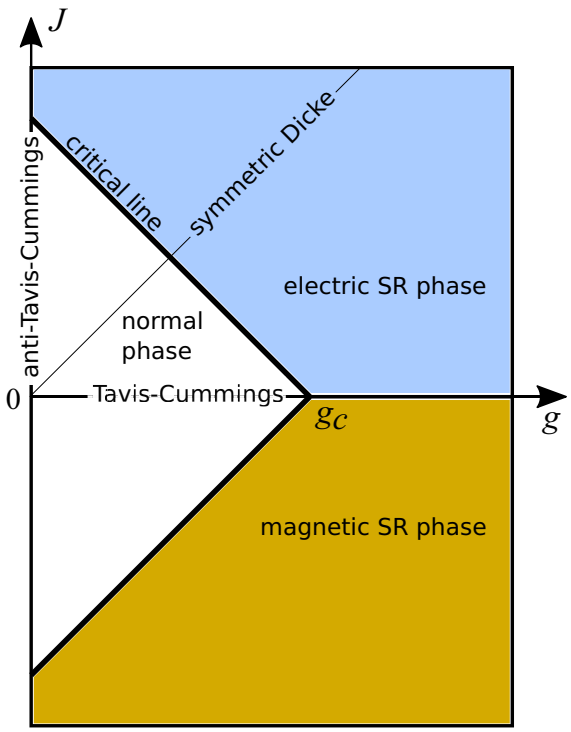

FIG. 1. Phase diagram of GDM for a thermodynamic limit of $N = \infty$. The horizontal (vertical) axis corresponds to TCM (anti-TCM); thin line $J = g$ corresponds to symmetric Dicke model. Critical lines, determined by the relation $g + |J| = g_c$, correspond to transitions from normal to "electric" ($J > 0$) or "magnetic" ($J < 0$) superradiant (SR) phases.

the normal-to-superradiant transition. Strictly speaking, we deal not with the phase transition in its conventional mean-field sense but with a fluctuational transition of a finite width. As for any critical region, a natural question on the corresponding fluctuational behavior arises. We show that the critical region has rather complicated internal structure, where relative fluctuations of photon number and field squeezing reveal different universal behaviors.

The paper is organized as follows. In Sec. II the problem formulation and path integral methodology are introduced. In Sec. III the results of the work are presented: relative fluctuations, Fano factor, and squeezing parameters are discussed in Sec. III A, minimal temperature scales of our theory are found in Sec. III B, and alternative approach based on Bethe ansatz is introduced in Sec. III C. In Sec. IV we discuss our results and in Sec. V we summarize.

II. METHODOLOGY

A. Problem formulation

Eigenfunctions of the model (1) have an infinitely entangled structure due to discrete $\mathbb{Z}_2$ symmetry when g and J are simultaneously nonzero. In this case there is only conservation of the parity of total excitations number. The Hamiltonian commutes with the parity operator $\hat{\Pi} = \exp[i\pi\hat{M}_+]$ where $\hat{M}_+ = \hat{a}^\dagger\hat{a} + \frac{1}{2}\hat{S}^z$ is the operator of the total excitations number. However, there are two particular limits where the Hamiltonian possesses a continuous $U(1)$ symmetry and becomes

integrable. The first case is TCM, realized when $J = 0$ and $g \neq 0$. Here $\hat{H}$ conserves total excitations number, i.e., $\hat{H}$ and $\hat{M}_+$ commute. The second case is the anti-Tavis-Cummings model (anti-TCM), realized when $g = 0$ and $J \neq 0$. This is nothing but opposite to RWA limit when the only antiresonant term appears in (1). The corresponding $\hat{H}$ conserves the excitation number difference defined through the operator $\hat{M}_- = \hat{a}^\dagger\hat{a} - \frac{1}{2}\hat{S}^z$. Here $[\hat{H}, \hat{M}_-] = 0$ and this is another type of continuous $U(1)$ symmetry.

Interaction parameters are assumed to be non-negative throughout the paper, $g \geqslant 0$ and $J \geqslant 0$, hence we address the superradiant phase of electric type according to Ref. [20] (see Fig. 1).

In superradiant phase a respective symmetry of $\hat{H}$, $\mathbb{Z}_2$, or $U(1)$ is broken and photons form a superradiant condensate. In the thermodynamic limit, the critical line of the phase transition is $g + J = g_c$. For $N \neq \infty$ the critical line is smeared into a fluctuational region of finite width where an average photon number changes smoothly. We are focused on equilibrium properties of a photon condensate into this critical region and analyze a relative fluctuations parameter

$$r = \frac{\langle\langle(\hat{a}^\dagger\hat{a})^2\rangle\rangle_\beta}{\langle\hat{a}^\dagger\hat{a}\rangle_\beta^2}, \tag{2}$$

Fano factor

$$F = \frac{\langle\langle(\hat{a}^\dagger\hat{a})^2\rangle\rangle_\beta}{\langle\hat{a}^\dagger\hat{a}\rangle_\beta}, \tag{3}$$

and squeezing parameters

$$\delta x = \frac{1}{2}\sqrt{\langle\langle\hat{x}^2\rangle\rangle_\beta}, \quad \delta p = \frac{1}{2}\sqrt{\langle\langle\hat{p}^2\rangle\rangle_\beta}. \tag{4}$$

The canonical coordinate $\hat{x} = (\hat{a}^\dagger + \hat{a})/\sqrt{2}$ and momentum $\hat{p} = i(\hat{a}^\dagger - \hat{a})/\sqrt{2}$ correspond to electric and magnetic fields. Here $\langle\hat{O}\rangle_\beta = \mathrm{Tr}[\hat{O}e^{-\beta\hat{H}}]/\mathrm{Tr}[e^{-\beta\hat{H}}]$ denotes thermodynamical averaging, where $e^{-\beta\hat{H}}$ is equilibrium density matrix, $\beta = 1/T$, and fluctuations $\langle\langle\hat{O}\rangle\rangle_\beta = \langle\hat{O}^2\rangle_\beta - \langle\hat{O}\rangle_\beta^2$.

In our approach, thermodynamic averages are calculated by means of a path integral and Matsubara effective action. The action is formulated for complex boson field ψ_τ defined on imaginary time $\tau \in [0;\ \beta]$. This field and its conjugate $\bar{\psi}_\tau$ correspond to operators $\hat{a}$ and $\hat{a}^\dagger$, respectively. As known from previous works [23,24], zero Matsubara mode ψ_0, which is a complex variable, parametrizes a superradiant order parameter. It can be represented as $\psi_0 = \sqrt{\Phi}e^{i\varphi}$ where Φ and φ are real variables in a path integral. They have a transparent meaning: the magnitude Φ is related to a photon number in the condensate, and φ is the order parameter complex phase. The zero-frequency mode is highlighted relative to others because it corresponds to a spontaneously emergent nonzero average of the photon field. The Goldstone effective potential $S[\bar{\psi}_0; \psi]$ for $U(1)$ case is shown in Fig. 2(a); blue dots and the variance $2\sqrt{\langle\Phi\rangle}$ correspond to a numerical simulation of random ψ_0 distributed with the probability density $\propto e^{-S[\bar{\psi}_0;\psi]}$.

A consequence of $\mathbb{Z}_2$ symmetry is that fluctuations of Φ and φ are governed by a non-Goldstone effective potential as shown in Fig. 2(b). Hence, relative fluctuations in the critical region are determined not only by fluctuations of Φ, as that in $U(1)$ TCM [27], but also by fluctuations of the condensate's phase which gives a nontrivial contribution. For instance, in $U(1)$ case the squeezing is absent, while it appears in the generalized model under consideration. The effect of squeezing and respective parameter δp are illustrated in Fig. 2(b) for the random distribution of ψ_0.

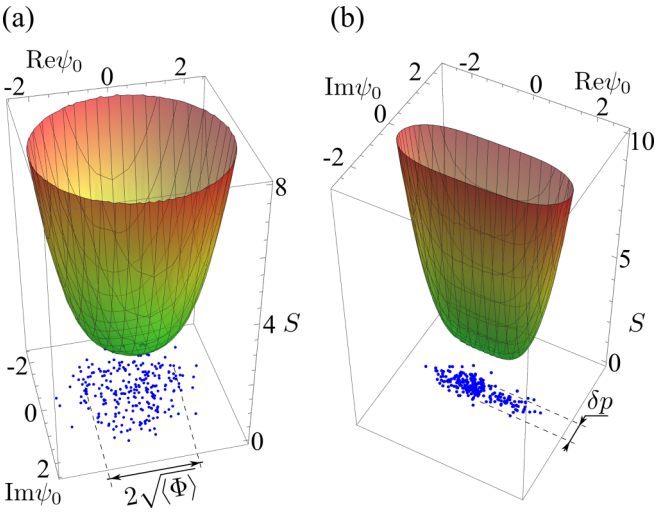

FIG. 2. Effective potential S for condensate mode ψ_0 at the critical point of the superradiant phase transition. (a) $U(1)$ case of TCM with Goldstone potential. (b) $\mathbb{Z}_2$ case of GDM with non-Goldstone potential. 250 blue dots in each panel correspond to numerical simulation of a random realization of ψ_0 with the respective S. The variance of the random ψ_0 in TCM is given by the average photon number as $2\sqrt{\langle\Phi\rangle}$, the squeezing in GDM is shown as δp; their expressions are given in (50) and (73). Parameters of the simulation: $N = 50$, temperature $T = \omega/10$, $\epsilon = \omega$, $J = 0$, and $g = g_c$ in (a), and $J = g = g_c/2$ in (b).

According to Ref. [27], TCM has universal value of $r = \frac{\pi}{2} - 1$ at the critical region; its width is determined by the scale $\Delta = \sqrt{\omega T/N}$. The Fano factor was shown to have a peak with the value much greater than unity $F \gg 1$, which indicates strongly positive correlations between photons at the phase transition. In normal and superradiant phases, however, $F < 1$ and the correlations are negative (antibunching effect). In this work we analyze how r and F change if antiresonant J appears in the model. Figure 3 shows the phase diagram of the model (1) with antiresonant terms and finite N and T. The critical region of the interest corresponds to the colored area (here $F > 1$ and the width is also determined by Δ). The effective theory presented allows us to analyze a behavior inside the critical region and describe fluctuations in TCM, anti-TCM, and GDM sectors, as well as in crossovers between them.

B. Total action

In this part we introduce total action of a hybrid system at equilibrium described by the Hamiltonian (1). As indicated above, when we formulate the path integral technique, the photon mode is represented via boson complex field ψ. However, Pauli operators can be parametrized in different ways in path integrals. This can be the Holstein-Primakoff bosonization which provides an exact diagonalization of the symmetric

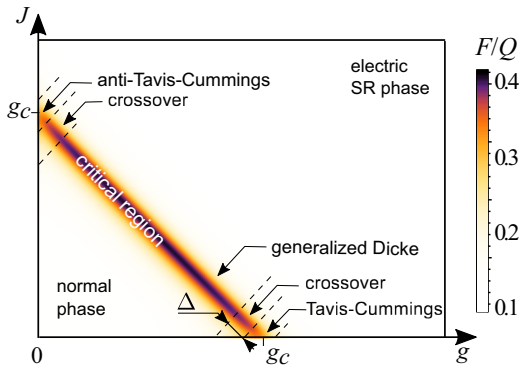

FIG. 3. Phase diagram of GDM at finite $N = 50$, temperature $T = \omega/10$, and $\epsilon = \omega$. The Fano factor $F(g, J)$ normalized by $\mathcal{Q} = \sqrt{NT\epsilon/\omega^2}$ is plotted. Normal phase and electric superradiant phase (white regions) are mediated by the critical region of the width $\Delta = \sqrt{\omega T/N}$ (colored area near the line $g + J = g_c$). TCM and anti-TCM sectors, where the Fano factor takes universal ratio $F_{\rm TC}/\mathcal{Q} = \frac{\sqrt{\pi}}{2} - \frac{1}{\sqrt{\pi}} \approx 0.32204$, and crossovers sectors are also determined by Δ. In the GDM sector, which covers the major part of the critical region, the universal ratio is $F_{\rm GD}/\mathcal{Q} = \frac{\Gamma(5/4)}{\Gamma(3/4)} - \frac{\Gamma(3/4)}{4\Gamma(5/4)} \approx 0.40168$.

Dicke model in the thermodynamic limit [29]. Alternatively to the bosonization, there are several fermion representations. For instance, Pauli operators can be parametrized via bilinear forms of semi-fermion fields [23]. These are Grassmann fields with unconventional boundary conditions on the imaginary time axis. Another example is a combination of conventional fermions where an auxiliary boson field is introduced in order to preserve the correct dimensionality of the Hilbert space [24].

In our approach we choose Majorana fermion representation of Pauli operators [39–41]. As shown in Ref. [27] for TCM, this method is rather convenient for analysis of a fluctuational behavior near the phase transition.

The Majorana representation of Pauli operator for the jth qubit is defined through the bilinear form of a conventional (complex) fermion operator $\hat{c}_j \neq \hat{c}_j^\dagger$ and Majorana one $\hat{d}_j = \hat{d}_j^\dagger$,

$$\hat{\sigma}_j^+ = \sqrt{2}\hat{c}_j^\dagger \hat{d}_j, \quad \hat{\sigma}_j^- = \sqrt{2}\hat{d}_j \hat{c}_j. \tag{5}$$

The Majorana mode has zero energy with the average $\langle \hat{d}_j^2 \rangle_\beta = 1/2$, while the complex fermion has energy ϵ_j. The partition function as a path integral reads as

$$Z = \int \mathcal{D}[\Psi, \mathcal{C}] \exp(-S_{\rm tot}[\Psi, \mathcal{C}]), \tag{6}$$

where complex boson variables are collected in the vector

$$\Psi_\tau^T(\tau) = [\bar{\psi}(\tau), \psi(\tau)] \tag{7}$$

and independent Grassmann variables, which parametrize fermion operators $\hat{c}_j^\dagger$, $\hat{c}_j$, and $\hat{d}_j$, are collected in the vector

$$\mathcal{C}^T(\tau) = \{\bar{c}_j(\tau), c_j(\tau), d_j(\tau)\}_{j=1}^N. \tag{8}$$

Total Matsubara action is

$$S_{\rm tot}[\Psi, \mathcal{C}] = S_{\rm ph}[\Psi] + S_\sigma[\mathcal{C}] + S_{\rm int}[\Psi, \mathcal{C}] + \ln Z_{\rm ph} Z_\sigma. \tag{9}$$

The first term here is the free photon mode's action

$$S_{\rm ph}[\Psi] = \beta \sum_n \bar{\psi}_n \big(- G_{{\rm ph};n}^{-1} \big) \psi_n, \tag{10}$$

where the respective bosonic Green function is

$$G_{{\rm ph};n}^{-1} = i2\pi nT - \omega. \tag{11}$$

The Matsubara modes ψ_n with $n \in \mathbb{Z}$ here are given by a discrete Fourier transformation on imaginary time interval

$$\psi_n = T \int_0^\beta \psi(\tau) e^{i2\pi nT\tau} d\tau,$$
$$\bar{\psi}_n = T \int_0^\beta \bar{\psi}(\tau) e^{-i2\pi nT\tau} d\tau. \tag{12}$$

They correspond to bosonic frequencies $2\pi nT$. The same transformation applies for fermion modes with odd frequencies $(2\pi n + \pi)T$.

The second term in (9) is the Majorana representation of two-level systems' action

$$S_\sigma[\mathcal{C}] = \frac{1}{2} \sum_{j=1}^N \sum_n \mathcal{C}_{j;-n}^T \big(- \mathbf{G}_n^{-1} \big) \mathcal{C}_{j;n}, \tag{13}$$

where the inverse fermion Green function has the following matrix structure:

$$\mathbf{G}_n^{-1} = \begin{bmatrix} 0 & i(2n+1)\pi T - \epsilon & 0 \\ i(2n+1)\pi T + \epsilon & 0 & 0 \\ 0 & 0 & i(2n+1)\pi T \end{bmatrix}$$

and acts on the vectors composed of Matsubara modes $\mathcal{C}_{j;n} = [\bar{c}_{j;-n}; c_{j;n}; d_{j;n}]^T$.

The third term in (9) is the interaction

$$S_{\rm int}[\Psi, \mathcal{C}] = \frac{1}{\sqrt{2}} \sum_{j=1}^N \sum_{m,k} \mathcal{C}_{j;-m}^T \mathbf{V}_{m-k} \mathcal{C}_{j;k} \tag{14}$$

represented via the matrix $\mathbf{V}$ involving complex boson fields as its elements:

$$\mathbf{V}_n = \begin{bmatrix} 0 & 0 & g\bar{\psi}_{-n} + J\psi_n \\ 0 & 0 & -(g\psi_n + J\bar{\psi}_{-n}) \\ -(g\bar{\psi}_{-n} + J\psi_n) & g\psi_n + J\bar{\psi}_{-n} & 0 \end{bmatrix}.$$

Note that m and k indices in (14) stand for fermionic frequencies $(2\pi m + \pi)T$ and $(2\pi k + \pi)T$, while their difference in $\mathbf{V}_{m-k}$ stands for the bosonic one $2\pi(m-k)T$.

The last term in (9) provides the unity normalization of Z for a noninteracting limit $g = J = 0$. The partition functions of free photon mode $Z_{\rm ph} = \prod_n (-G_{{\rm ph};n})$, and isolated N two-level systems $Z_\sigma = \prod_n [\mathrm{Det}\,(-\mathbf{G}_n)]^{-N/2}$, are given by infinite products over Matsubara modes, as follows from Gaussian

integration rules. They read as

$$\int D[\bar{\Psi},\Psi]e^{-\bar{\Psi}A\Psi} = \int\prod_n \frac{d\bar{\psi}_n d\psi_n}{\pi}\exp\left[-\sum_{n,m}\bar{\psi}_n A_{n,m}\psi_m\right] = \frac{1}{\mathrm{Det}\,A}, \tag{15}$$

for complex variables (the matrix A has non-negative eigenvalues). For nonindependent Grassmann variables with an antisymmetric matrix $\mathcal{A}$ we have

$$\int D[\mathcal{C}]e^{-\frac{1}{2}\mathcal{C}^T\mathcal{A}\mathcal{C}} = \int\prod_{j;n} d\bar{c}_{j;n}dc_{j;n}dd_{j;n}\exp\left[-\frac{1}{2}\sum_{j;n,m}\mathcal{C}_{j;n}\mathcal{A}_{j;n,m}\mathcal{C}_{j;m}\right] = \sqrt{\mathrm{Det}\,\mathcal{A}}. \tag{16}$$

C. Effective functional for photon mode fluctuations

In this part an effective action for equilibrium photon mode is derived. We start from Gaussian integration over $\mathcal{C}$ fields with the use of the identity (16) equivalent to taking a trace over the Hilbert space of two-level systems. Applying the identity

$$\ln\mathrm{Det}\,\mathcal{A} = \mathrm{Tr}\ln\mathcal{A}, \tag{17}$$

we arrive at the effective action in a general form $S_{\mathrm{eff}}[\Psi] = S_{\mathrm{ph}}[\Psi] + \ln Z_{\mathrm{ph}}Z_\sigma - \frac{1}{2}N\mathrm{Tr}\ln(-\mathbf{G}^{-1}+\mathbf{V})$, which, after a standard resummation of the logarithm, becomes

$$S_{\mathrm{eff}}[\Psi] = S_{\mathrm{ph}}[\Psi] + \ln Z_{\mathrm{ph}}\sqrt{Z_\sigma} - \frac{1}{4}N\mathrm{Tr}\ln\left[-\delta_{n,m}\mathbf{G}_m^{-1} + \sum_l \mathbf{V}_{n-l}\mathbf{G}_l\mathbf{V}_{l-m}\right]. \tag{18}$$

To obtain the effective functional from (18) describing the superradiant phase transition and fluctuations above the photon condensate, we separate zero mode from the others in the self-energy matrix as

$$\sum_l \mathbf{V}_{n-l}\mathbf{G}_{j;l}\mathbf{V}_{l-m} = \delta_{n,m}\mathbf{V}_0\mathbf{G}_m\mathbf{V}_0 + \sum_{l\neq n,m}\mathbf{V}_{n-l}\mathbf{G}_{j;l}\mathbf{V}_{l-m} + (1-\delta_{n,m})(\mathbf{V}_{n-m}\mathbf{G}_m\mathbf{V}_0 + \mathbf{V}_0\mathbf{G}_n\mathbf{V}_{n-m}). \tag{19}$$

The first term depends on zero mode ψ_0 only, while the second term is a nondiagonal matrix that is determined by nonzero modes $\psi_{n\neq 0}$ which describe quasiparticle fluctuations above the condensate. The third term is a product of zero and nonzero Matsubara modes; it cancels out in further calculations.

At this step we introduce new fermion Green function which absorbs the diagonal part as

$$\mathcal{G}_{j;m}[\bar{\psi}_0,\psi_0] = \left[\mathbf{G}_{j;m}^{-1} - \mathbf{V}_0\mathbf{G}_{j;m}\mathbf{V}_0\right]^{-1} \tag{20}$$

and expand the logarithm in $S_{\mathrm{eff}}[\Psi]$ by a first order in the nondiagonal part of **VGV**:

$$\ln\sqrt{Z_\sigma} - \frac{1}{4}N\mathrm{Tr}\ln\left[-\delta_{n,m}\mathbf{G}_m^{-1} + \sum_l \mathbf{V}_{n-l}\mathbf{G}_l\mathbf{V}_{l-m}\right] \approx -\frac{1}{4}\mathrm{Tr}\ln\left(\mathbf{G}_{j;m}\mathcal{G}_{j;m}^{-1}[\bar{\psi}_0,\psi_0]\right) + \frac{1}{4}N\mathrm{Tr}\left[\mathcal{G}_{j;n}[\bar{\psi}_0,\psi_0]\sum_{l\neq n,m}\mathbf{V}_{n-l}\mathbf{G}_{j;l}\mathbf{V}_{l-m}\right]. \tag{21}$$

Here we use the assumption that quasiparticle fluctuations $\psi_{n\neq 0}$ are sufficiently small.

The effective action takes the following form after the expansion (21):

$$S_{\mathrm{eff}}[\Psi] \approx S[\bar{\psi}_0;\psi_0] + S_{\mathrm{fl}}[\bar{\psi}_{n\neq 0};\psi_{n\neq 0}] + \ln Z_{\mathrm{ph}}. \tag{22}$$

The first term is the functional for superradiant condensate

$$S[\bar{\psi}_0;\psi_0] = -\beta G_{\mathrm{ph};0}^{-1}|\psi_0|^2 - N\ln\frac{\cosh\frac{\sqrt{\epsilon^2+4|g\psi_0+J\bar{\psi}_0|^2/N}}{2T}}{\cosh\frac{\epsilon}{2T}}. \tag{23}$$

The logarithmic term here is a result of a calculation of $\mathrm{Tr}\ln(\mathbf{G}\mathcal{G}^{-1}[\bar{\psi}_0,\psi_0])$ in the second line of (21), where the trace is reduced to a calculation of the infinite product over fermion Matsubara modes. The functional (23) is of a non-Goldstone type due to a dependence on a complex phase of ψ_0.

The second term in (22) is responsible for Gaussian fluctuations above the condensate

$$S_{\mathrm{fl}}[\bar{\psi}_{n\neq 0};\psi_{n\neq 0}] = \frac{\beta}{2}\sum_{n\neq 0}\Psi_{-n}^T(-G_{\mathrm{fl};n}^{-1}[\bar{\psi}_0;\psi_0])\Psi_n, \tag{24}$$

where $\Psi_n^T = [\psi_n, \bar{\psi}_{-n}]$. The inverse Green function matrix $G_{\mathrm{fl};n}^{-1}[\bar{\psi}_0;\psi_0]$ involves self-energy given by the last term in (21). Formally, this self-energy does depend on the zero mode variable. However, such a dependence provides small by $1/N$ corrections when the system is near the critical region. Consequently, ψ_0 dependence can be neglected and we suggest $G_{\mathrm{fl};n}^{-1} = G_{\mathrm{fl};n}^{-1}[\bar{\psi}_0{=}\psi_0{=}0]$ where

$$G_{\mathrm{fl};n}^{-1} = \begin{bmatrix} -gJ(\Sigma_n+\Sigma_{-n}) & G_{\mathrm{ph};n}^{-1} - (g^2\Sigma_{-n}+J^2\Sigma_n) \\ G_{\mathrm{ph};n}^{-1} - (g^2\Sigma_n+J^2\Sigma_{-n}) & -gJ(\Sigma_n+\Sigma_{-n}) \end{bmatrix}. \tag{25}$$

Self-energies are parametrized by

$$\Sigma_n = \frac{\tanh\frac{\epsilon}{2T}}{2i\pi nT - \epsilon} \tag{26}$$

which coincides with a self-energy in RWA.

Note that the condensate functional $S[\bar{\psi}_0;\psi_0]$ is symmetric under the interchange of g and J, however, model (1) does not have this symmetry for $\epsilon \neq 0$. As it should be, this asymmetry is recovered in the total action $S_{\mathrm{eff}}[\Psi]$ which involves excitations above the condensate encoded by nonzero modes. It can be seen from $S_{\mathrm{fl}}[\bar{\psi}_{n\neq 0};\psi_{n\neq 0}]$, where $G_{\mathrm{fl};n}^{-1}$ is not symmetric under the interchange of g and J. Namely, the asymmetry follows from $\Sigma_n \neq \Sigma_{-n}$ for any $\epsilon \neq 0$.

D. Effective action for condensate magnitude

As long as we address the critical region near the superradiant transition, the leading contribution to fluctuational behavior comes from the photon condensate. Hence, calculations of the thermodynamical average is reduced to a path integral with the only one complex variable ψ_0. As mentioned before, we parametrize it as

$$\psi_0 = \sqrt{\Phi} e^{i\varphi}, \tag{27}$$

where $\Phi = |\psi_0|^2$ is the magnitude of superradiant order parameter and φ is its phase. Both Φ and φ are quantum variables fluctuating in the potential

$$S[\Phi,\varphi] = \frac{\omega}{T}\Phi + N \ln\cosh\frac{\epsilon}{2T} - N\ln\cosh \times \left[\frac{\epsilon}{2T}\sqrt{1+\frac{4\Phi}{N\epsilon^2}(g^2+J^2+2gJ\cos 2\varphi)}\right]. \tag{28}$$

We study hereafter a behavior at temperatures $T \ll \epsilon$, where the condensate functional (28) is reduced to the following form:

$$S[\phi,\varphi] = \phi - \frac{1}{2\gamma}(\sqrt{1+4\gamma\eta[\varphi]\phi}-1),$$
$$\eta[\varphi] = \eta_0 - 2\eta_1\sin^2\varphi, \tag{29}$$

where $\phi = \beta\omega\Phi$ is rescaled order parameter and $\eta[\varphi]$ determines phase dependence. The dimensionless interaction parameters in (29) read

$$\eta_0 = \frac{(g+J)^2}{\epsilon\omega}, \tag{30}$$
$$\eta_1 = \tfrac{2gJ}{\epsilon\omega}, \tag{31}$$

and rescaled temperature

$$\gamma = \frac{T}{N\epsilon} \tag{32}$$

is a small parameter of our theory $\gamma \ll 1$. A remarkable property of the action (29) is that γ appears twice as a denominator in $\frac{1}{2\gamma}$ and as a prefactor in the square root term. This property allows us to extract the relevant part of the action $S[\phi,\varphi]$ within three steps.

The first step is an expansion of the square root by small γ up to second order. Here we assume that phase and magnitude are such that the condition $\gamma\eta[\varphi]\phi \ll 1$ is fulfilled. Note, the presence of the overall $\frac{1}{2\gamma}$ prefactor in (29) reduces the order of γ in this expansion and the action at this point reads as $S[\phi,\varphi] = (1-\eta[\varphi])\phi + \gamma\eta^2[\varphi]\phi^2$. In particular, γ cancels out in front of the linear in ϕ term $(1-\eta[\varphi])\phi$; this fact is crucial for further analysis. At the phase transition, the relevant values of phase are such that $\eta[\varphi] \sim 1$; hence path integrals over ϕ converge in the domain $0 < \phi \lesssim \gamma^{-1/2}$. This means that the initial condition $\gamma\eta[\varphi]\phi \ll 1$ is always satisfied and γ expansion is strict.

The second step is to neglect φ dependence in the quadratic term $\gamma\eta^2[\varphi]\phi^2$ and replace it by $\gamma\eta_0^2\phi^2$. Here the phase is replaced by its value at the functional minima ($\varphi = 0$ and $\varphi = \pi$) where $\sin\varphi = 0$. The result of the above two step reads

$$S[\phi,\varphi] = (1-\eta_0+2\eta_1\sin^2\varphi)\phi + \gamma\eta_0^2\phi^2. \tag{33}$$

The third step of our derivation is the integrating out the phase φ from the action (33). This is performed exactly with the use of the identity

$$\int_0^{2\pi} e^{-2z\sin^2\varphi} d\varphi = 2\pi e^{-z} I_0(z), \tag{34}$$

where $z = \eta_1\phi$ and $I_0(z)$ is a modified Bessel function of zero order. Ascending the result of integration into the exponent, we arrive at one of the central results of this work, the action for photon condensate magnitude:

$$S_\phi = (1-\eta_0+\eta_1)\phi + \gamma\eta_0^2\phi^2 - \ln I_0(\eta_1\phi). \tag{35}$$

The modified Bessel function logarithm $\ln I_0(\eta_1\phi)$ describes the dissipative dynamics of ϕ due to a coupling between the fluctuations of the density of photon condensate and its phase.

It is important that the small parameter γ does not enter into the dissipative term (35). Instead, γ appears in quadratic term only and provides a width of Gaussian tails $\phi \sim 1/\sqrt{\gamma}$ in the partition function exponent. It means that a character argument of the Bessel function is estimated as $z = \eta_1/\sqrt{\gamma}$ in this case. It can be both small or large compared to unity ($z \ll 1$ and $z \gg 1$), depending on the interaction parameters. Consequently, different asymptotic expansions can be applied for $\ln I_0(z)$. To the best of our knowledge, properties of this action has not yet been studied in GDM context and our work is devoted to this issue.

E. Expressions for *r*, *F*, and squeezing parameters

Before we proceed with asymptotic expansions of the dissipative term, let us make a step back to definitions for r, F, and squeezing parameters. According to the path integral approach indicated above, thermodynamical average of a certain operator $\mathcal{F}[\hat{a},\hat{a}^\dagger]$ is represented via integrals over the condensate variables Φ and φ. Hereafter, this double integral is denoted as $\langle\ \rangle$ brackets without a subscript, and thermodynamical average then becomes

$$\langle\mathcal{F}[\hat{a},\hat{a}^\dagger]\rangle_\beta = \langle\tilde{\mathcal{F}}[\Phi,\varphi]\rangle,$$
$$\langle\tilde{\mathcal{F}}[\Phi,\varphi]\rangle \equiv Z_0^{-1}\int_0^\infty d\Phi\int_0^{2\pi} d\varphi\ \tilde{\mathcal{F}}[\Phi,\varphi]e^{-S[\Phi,\varphi]}. \tag{36}$$

Here $\mathcal{F}$ transforms into $\tilde{\mathcal{F}}$ under the parametrization of ψ_0 through Φ and φ, and Z_0 is the normalization factor providing $\langle 1\rangle = 1$. The same definition (36) applies for thermodynamic fluctuations: $\langle\langle\mathcal{F}\rangle\rangle_\beta = \langle\langle\tilde{\mathcal{F}}\rangle\rangle$ with $\langle\langle\tilde{\mathcal{F}}\rangle\rangle \equiv \langle\tilde{\mathcal{F}}^2\rangle - \langle\tilde{\mathcal{F}}\rangle^2$. Namely, the average and fluctuations of photon numbers, i.e., their first and second cumulants, have the following forms:

$$\langle\hat{a}^\dagger\hat{a}\rangle_\beta = \langle\Phi\rangle, \quad \langle\langle(\hat{a}^\dagger\hat{a})^2\rangle\rangle_\beta = \langle\langle\Phi^2\rangle\rangle. \tag{37}$$

From a technical point of view we use the effective functional for rescaled order parameter (35) in the calculation of the photon number moments:

$$\langle\Phi^k\rangle = \frac{\int_0^\infty \phi^k e^{-S_\phi} d\phi}{(\beta\omega)^k\int_0^\infty e^{-S_\phi} d\phi}. \tag{38}$$

The representation (38) is used in calculation of r and F parameters.

The electric and magnetic fields operators in Φ-φ representation become

$$\frac{\hat{a}^\dagger + \hat{a}}{\sqrt{2}} \to \sqrt{2\Phi}\cos\varphi \tag{39}$$

and

$$i\frac{\hat{a}^\dagger - \hat{a}}{\sqrt{2}} \to \sqrt{2\Phi}\sin\varphi, \tag{40}$$

respectively. First cumulants of these fields equal zero, $\langle\sqrt{\Phi}\cos\varphi\rangle = \langle\sqrt{\Phi}\sin\varphi\rangle = 0$, due to π periodicity of the $S[\Phi,\varphi]$ functional. As a consequence, second cumulants of δx and δp coincide with the respective second moments. The expressions for squeezing parameters (4) in Φ-φ representation become averages of the fields quadratures (39) and (40):

$$\delta x = \sqrt{\langle\Phi\cos^2\varphi\rangle}, \quad \delta p = \sqrt{\langle\Phi\sin^2\varphi\rangle}. \tag{41}$$

Calculation of the squeezing parameters (41) is based on $S[\phi,\varphi]$ from (33). The integration over φ is performed analytically and expressions for δx and δp are represented as ϕ integrals:

$$\begin{aligned}\delta x &= \left[\frac{\int_0^\infty \phi\left(1+\frac{I_1(\eta_1\phi)}{I_0(\eta_1\phi)}\right)e^{-S_\phi}d\phi}{2\beta\omega\int_0^\infty e^{-S_\phi}d\phi}\right]^{1/2},\\ \delta p &= \left[\frac{\int_0^\infty \phi\left(1-\frac{I_1(\eta_1\phi)}{I_0(\eta_1\phi)}\right)e^{-S_\phi}d\phi}{2\beta\omega\int_0^\infty e^{-S_\phi}d\phi}\right]^{1/2}.\end{aligned} \tag{42}$$

It should be noted, the higher-order corrections due to nonzero modes $\psi_{n\neq 0}$ are neglected here by small parameter T^*/T, where T^* is a minimal temperature scale where our theory can be applied, i.e., when the first-order expansion in (22) is correct. We discuss this issue in more detail in Sec. III B.

III. RESULTS

A. Universal fluctuations at the critical region

Depending on a value of η_1, there are different universal behaviors of fluctuations at the phase transition. They are dictated by the dissipative term $\ln I_0(\eta_1\phi)$ in the action S_ϕ. As mentioned above, the relevant values of ϕ, where the path integrals (38) and (42) converge, are determined by the scale of $\gamma^{-1/2}$. Introducing a parameter $z = \eta_1\gamma^{-1/2}$ as a typical scale of the dissipative term argument, there are different asymptotics of $\ln I_0(\eta_1\phi)$. We address the important limits of small $z \ll 1$ and large $z \gg 1$ parameters.

As shown below, the limit of $z \ll 1$ corresponds to TCM and anti-TCM regimes (see Fig. 3) where the antiresonant interaction is effectively suppressed by thermal fluctuations. Oppositely, $z \gg 1$ is related to GDM where antiresonant interaction becomes relevant. Also, an intermediate regime of $z \sim 1$ is analyzed; it corresponds to a crossover between universal behaviors of TCM and GDM located inside the critical region.

1. Anti-Tavis-Cummings and Tavis-Cummings regimes

Here we address the $z \ll 1$ asymptotic of (35), in other words, the limit of small antiresonant interaction $\eta_1 \ll \sqrt{\gamma} \ll 1$. This range determines the interaction parameters near the point $\eta_1 = 0$, which, according to (31), corresponds to $U(1)$ limits of anti-TCM and TCM. Note that these models reveal identical structures of condensate functionals. As mentioned above, this fact is a consequence of the consideration limited by zero mode only.

The small argument expansion for the dissipative term up to fourth order is

$$\ln I_0(z \ll 1) \approx \frac{1}{4}z^2 - \frac{1}{64}z^4. \tag{43}$$

Hence, one arrives at the following expression:

$$S_\phi = (1 - \eta_0 + \eta_1)\phi + \left(\gamma\eta_0 - \frac{\eta_1^2}{4}\right)\phi^2 + \frac{\eta_1^4}{64}\phi^4. \tag{44}$$

It is important to note that contributions of third and fourth orders by ϕ also appear in the square root expansion of (29), however, they are small by γ compared to those given by $\ln I_0(\eta_1\phi)$ and, hence, are neglected.

The action (44) describes second-order phase transition if the parameters satisfy

$$\eta_0 - \eta_1 = 1. \tag{45}$$

In dimensional units, the critical condition (45) determines a critical line as a circle of the radius g_c: $g^2 + J^2 = g_c^2$. However, the initial condition on small $\eta_1 \ll \sqrt{\gamma}$ leaves narrow regions from this circle on a phase diagram: TCM behavior is realized when $g = g_c$ and antiresonant coupling is limited as $J \ll \Delta$, where

$$\Delta = \sqrt{\frac{\omega T}{N}}. \tag{46}$$

For anti-TCM a dual condition holds: $g \ll \Delta$ and $J = g_c$.

The energy scale Δ plays a central role in our solution, because it determines an area inside the critical region where nonresonant terms are irrelevant, and also the width of the Ginzburg-Levanyuk fluctuational region of the normal-to-superradiant transition. The fact that this width is also equal to Δ is found from a matching condition $\gamma^{-1/2} \sim \phi_{\min}$. Here we match the width of the Gaussian integrand $\gamma^{-1/2}$ and the value of $\phi = \phi_{\min}$ where the functional (44) has a minimum and corresponds to the superradiant phase with $\eta_0 - \eta_1 > 1$,

$$\phi_{\min} = \frac{\eta_0 - \eta_1 - 1}{2\gamma}. \tag{47}$$

We note that a nonzero Δ appears only when T and $1/N$ are simultaneously nonzero. It vanishes as $\Delta \propto N^{-1/2}$ in the thermodynamic limit.

Let us find fluctuational parameters for these two areas (TCM and anti-TCM) of the critical region. As long as $\eta_1 \ll \sqrt{\gamma}$, one has $\eta_0 \approx 1$ according to (45) and the action (44) is reduced to Gaussian form

$$S_\phi = \gamma\phi^2. \tag{48}$$

From (48) we find the average photon number [it is illustrated in Fig. 2(a) for Goldstone potential]; in dimensional units

reads

$$\langle\Phi\rangle_{\rm TC} = \frac{1}{\sqrt{\pi}}\mathcal{Q}, \tag{49}$$

where we introduce scaling function

$$\mathcal{Q} = \frac{1}{\beta\omega\sqrt{\gamma}} = \left[\frac{NT\epsilon}{\omega^2}\right]^{1/2}, \tag{50}$$

which determines the photon number, fluctuations, and Fano factors. The assumption that the leading part in the photon number is provided by the condensate means $\mathcal{Q} \gg 1$. This gives a modification of low temperature constraint in the following form:

$$\epsilon \gg T \gg T^*_{\rm TC}, \tag{51}$$

where the minimal temperature is

$$T^*_{\rm TC} = \frac{\omega^2}{N\epsilon}. \tag{52}$$

In other words, our theory based on the condensate functional is applicable if a temperature is above T^*. For T less than T^* one has to include higher orders in the logarithm expansion of $S_{\rm eff}$, see Eq. (18). The fact that we cannot go down to arbitrary low temperatures is discussed in Sec. III B in more details.

Calculations with the Gaussian action (48) give the following result for relative fluctuations:

$$r_{\rm TC} = \frac{\pi}{2} - 1 \approx 0.57080, \tag{53}$$

and the universal ratio for Fano factor

$$F_{\rm TC}/\mathcal{Q} = \left(\frac{\sqrt{\pi}}{2} - \frac{1}{\sqrt{\pi}}\right) \approx 0.32204 \tag{54}$$

(they were previously obtained in Ref. [27]). In Fig. 4(b) $r(g)$ dependence near the critical point $g = g_c$ is plotted for $N = 50$ (black curve), $N = 200$ (blue curve), and $N = 800$ (red curve). The crossing of all the curves in the same point $r(g_c) = r_{\rm TC}$ demonstrates the universality of this parameter.

The squeezing parameters show that the condensate is slightly squeezed in p direction for a nonzero J:

$$\begin{aligned}\delta x_{\rm TC} &= \sqrt{\frac{\langle\Phi\rangle_{\rm TC}}{2}}\left(1 + \frac{J}{4}\sqrt{\frac{\pi N}{T\omega}}\right),\\ \delta p_{\rm TC} &= \sqrt{\frac{\langle\Phi\rangle_{\rm TC}}{2}}\left(1 - \frac{J}{4}\sqrt{\frac{\pi N}{T\omega}}\right).\end{aligned} \tag{55}$$

One obtains a small correction to 1/2 in fluctuations of the phase $\langle\sin^2\varphi\rangle_{\rm TC} = 1/2 - \frac{\eta_1}{4\sqrt{\pi\gamma}}$. In the dimensional units this is

$$\langle\sin^2\varphi\rangle_{\rm TC} = \frac{1}{2} - \frac{J}{2\sqrt{\pi T\omega}}. \tag{56}$$

For a definiteness we assumed TCM limit in the derivation of (56) and (55); anti-TCM results are the same as above with J replaced by g. A comparison of (55) and (56) shows that the difference between $\delta p_{\rm TC}$ and the factorized product $(\langle\Phi\rangle_{\rm TC}\langle\sin^2\varphi\rangle_{\rm TC})^{1/2}$ appears linear by J.

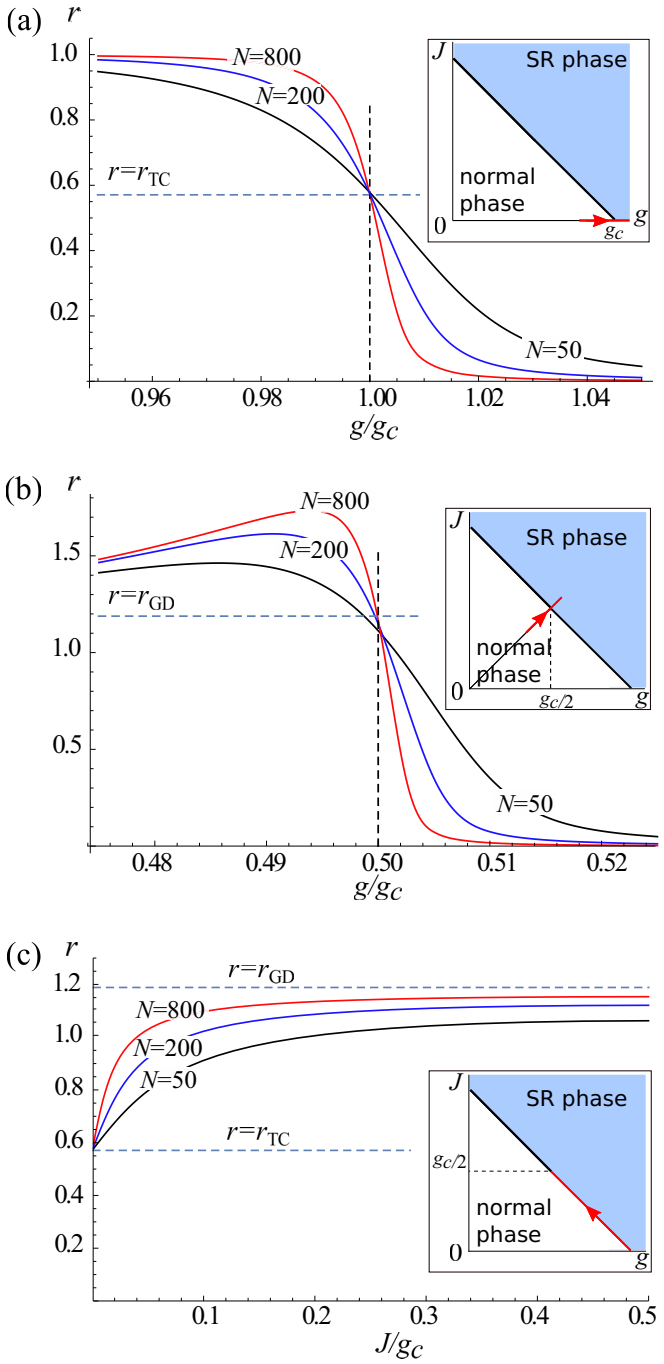

FIG. 4. Relative fluctuations r of photon condensate near superradiant phase transition as a function of interaction strengths. Insets: Red cut in the schematic phase diagram shows a curve in g and J parameter space for which r dependence is plotted. Parameters used in calculations: $\beta\omega = \beta\epsilon = 100$, three curves in each plot correspond to $N = 50$ (black), 200 (blue), and 800 (red). (a) Regime of TCM; crossing of curves $r(g)$ for different N near the critical point $g/g_c = 1$, where relative fluctuations take universal value $r_{\rm TC} = \frac{\pi}{2} - 1 \approx 0.57080$. (b) Regime of GDM, the symmetric case of $J = g$; crossing of $r(g)$ at the critical interaction $g/g_c = \frac{1}{2}$, where relative fluctuations take universal value $r_{\rm GD} = 4\frac{\Gamma^2(5/4)}{\Gamma^2(3/4)} - 1 \approx 1.18844$. (c) Dependence of r on antiresonant coupling strength $0 < J < g_c/2$ along the critical line $J + g = g_c$. Here $J = 0$ and $J/g_c = \frac{1}{2}$ correspond to TCM and symmetric Dicke model, respectively, and r evolves between two asymptotical values of $r_{\rm TC}$ and $r_{\rm GD}$.

2. Crossover regime

Here we analyze a special case of $\eta_1 = 2\sqrt{\gamma}$ when the system is near the superradiant phase transition. According to (45), it means that $\eta_0 = 1 - 2\sqrt{\gamma}$. This point corresponds to a case when antiresonant interaction J approaches Δ and TCM-to-GDM crossover occurs.

The quadratic part in the functional (44) vanishes at the crossover and it becomes quartic,

$$S_\phi = \frac{\gamma}{4}\phi^4. \tag{57}$$

Remarkably, scaling functions of photon number and their fluctuations found from the quartic action are the same as for TCM: $\langle\Phi\rangle^2 \sim \sqrt{\langle\langle\Phi^2\rangle\rangle} \sim \mathcal{Q}$. This is an important result we learn from the action (57). Another one is the universal behavior of fluctuations, in other words, the parameter r changes at TCM-to-GDM crossover; it follows from the change of S_ϕ to quartic structure. This is due to the different prefactors in front of $\mathcal{Q}$ in expressions for $\langle\Phi\rangle$ and $\sqrt{\langle\langle\Phi^2\rangle\rangle}$ calculated with (57). Note that accurate calculations of r and F require an inclusion of higher order terms in (57), because z is close to unity in the initial expansion (43) for $\ln I_0(z)$ at the crossover point.

This asymptotic behavior of S_ϕ is valid for small deviation of η_1 from $\eta_1 = 2\sqrt{\gamma}$ restricted by the condition $|2\sqrt{\gamma} - \eta_1| \ll \sqrt{\gamma}$. In dimensional units such a condition is equivalent to

$$|\Delta - J| \ll \Delta. \tag{58}$$

Of course, in thermodynamic limit we have $\Delta = 0$ and a smooth transition between $J = 0$ and $J \neq 0$ models no longer exists. A condition similar to (58) holds for g in the opposite limit of anti-TCM.

In our case, when N and T are finite, the matching condition $\Delta \sim J$ at the TCM-to-GDM crossover can be inverted. One finds a character crossover temperature

$$T_{\rm crs} = \frac{J^2 N}{\omega}. \tag{59}$$

The presence of weak antiresonant interaction J in $\hat{H}$ becomes irrelevant for $T > T_{\rm crs}$ and the system behaves according to the TCM model with the effective Goldstone functional (the same logic is applied for anti-TCM).

3. Generalized Dicke model regime. Squeezing

The third type of universal behavior at the critical region is provided by $z \gg 1$ and corresponds to $\mathbb{Z}_2$-GDM. Let us come back to the action (35) and approximate the modified Bessel function by its large argument asymptotics,

$$I_0(z \gg 1) = \frac{1}{\sqrt{2\pi z}} e^z. \tag{60}$$

As a result, we obtain for the effective action

$$S_\phi = (1 - \eta_0)\phi + \gamma\eta_0\phi^2 + \frac{1}{2}\ln\phi. \tag{61}$$

We note that the logarithmic divergence in (61) at $\phi = 0$ provides $\frac{1}{\sqrt{\phi}}$ singularity in a path integral if the logarithm is descended from the exponent. However, any of the moments $\langle\phi^k\rangle$ with $k \geqslant 0$ are integrable:

$$\langle\phi^k\rangle_{\rm GD} \sim \int_0^\infty \phi^k \frac{1}{\sqrt{\phi}} e^{-(1-\eta_0)\phi - \gamma\eta_0\phi^2} d\phi. \tag{62}$$

The representation (62) of the path integral restores a quadratic structure of the action, similarly to TCM, with the difference that the multiplier $\frac{1}{\sqrt{\phi}}$ appears in front of the exponent. This results in quantitative distinctions of fluctuational behavior from that studied for the TCM regime.

Let us determine the superradiant phase transition point in GDM via the exponent in representation (62). It follows from canceling of the linear in ϕ term:

$$\eta_0 = 1. \tag{63}$$

This critical point is different from that derived for TCM (45). At the critical point, another dimensionless interaction parameter belongs to the domain

$$\sqrt{\gamma} \ll \eta_1 < \frac{1}{2}, \tag{64}$$

where the upper bound $\eta_1 = 1/2$ corresponds to the critical point of the symmetric Dicke model with $g = J = g_c/2$. Reformulating (63) through g and J, we arrive at the critical line previously derived in Refs. [36,37]:

$$g + J = g_c. \tag{65}$$

According to the initial requirement of $\eta_1 \gg \sqrt{\gamma}$, the condition (65) is complemented by constraints $g \gg \Delta$ and $J \gg \Delta$ which means that we are beyond the TCM-to-GDM crossover. If one moves along $J = g$ direction in the phase diagram, then the width of the fluctuational region of the normal-to-superradiant transition is equal to Δ, the same as in the case of TCM.

The photon number in the GDM regime is

$$\langle\Phi\rangle_{\rm GD} = \frac{\Gamma(3/4)}{4\Gamma(5/4)}\mathcal{Q}, \tag{66}$$

with the same scaling function $\mathcal{Q}$ as that in $U(1)$ case (49) but different from $\frac{1}{\sqrt{\pi}} \approx 0.56419$ prefactor of $\frac{\Gamma(3/4)}{4\Gamma(5/4)} \approx 0.33799$. Here $\Gamma(y)$ is Euler gamma function which appears due to $\frac{1}{\sqrt{\phi}}$ term in path integrals (62). The relative fluctuations parameter is not $r = \frac{\pi}{2} - 1 \approx 0.57080$ anymore [see Eq. (53)], it takes another universal value

$$r_{\rm GD} = 4\frac{\Gamma^2(5/4)}{\Gamma^2(3/4)} - 1 \approx 1.18844. \tag{67}$$

This result means that relative fluctuations of the condensate are increased by the antiresonant interaction channel. The Fano factor, as in previous case (54), also scales with $\mathcal{Q}$, however, the prefactor in front is different and we find another universal ratio:

$$F_{\rm GD}/\mathcal{Q} = \frac{4\Gamma^2(5/4) - \Gamma^2(3/4)}{4\Gamma(5/4)\Gamma(3/4)} \approx 0.40168. \tag{68}$$

This ratio is greater than $F_{\rm TC}/\mathcal{Q} \approx 0.32204$ found for TCM which indicates that the photon bunching in the condensate becomes stronger.

In Fig. 4(b) a dependence of r for the symmetric Dicke model near critical point $g = J = g_c/2$ is plotted (see red cut

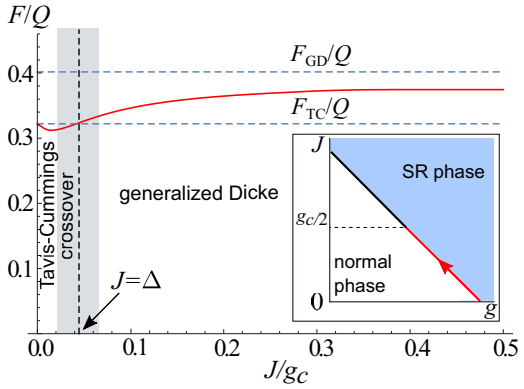

FIG. 5. Fano factor ratio $F/\mathcal{Q}$ as a function of antiresonant interaction J. The dependence is plotted for the half of the critical line, shown as red cut in the inset, where F is parametrized by antiresonant coupling strength $0<J<g_c/2$. $F/\mathcal{Q}$ evolves between two universal values of $F_{\rm TC}/\mathcal{Q}=\frac{\sqrt{\pi}}{2}-\frac{1}{\sqrt{\pi}}\approx 0.32204$ and $F_{\rm GD}/\mathcal{Q}=\frac{\Gamma(5/4)}{\Gamma(3/4)}-\frac{\Gamma(3/4)}{4\Gamma(5/4)}\approx 0.40168$ (shown as dashed blue lines). The vertical dashed line at $J=\Delta$ and shaded area nearby separate TCM and GDM regimes.

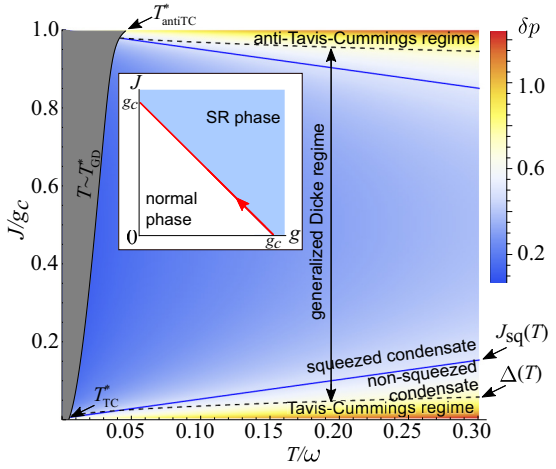

FIG. 6. Different regimes for δp squeezing in the critical region as a function of temperature T. Parameters g and J correspond to the red cut in the inset which covers the critical region entirely; the plot is parametrized by J (vertical axis). Blue lines $J=J_{\rm sq}(T)$ and $J=g_c-J_{\rm sq}(T)$ are boundaries between squeezed and nonsqueezed condensates. Dashed curves corresponds to crossovers between anti-TCM and TCM and GDM regimes. The gray sector is the part of phase diagram where quantum fluctuations due to nonzero Matsubara modes are important. Here our solution based on the effective functional for condensate modes only is not strict. The edge curve of the gray sector demonstrates schematically a dependence of minimal temperature on J. Its value is minimal near $J=0$, where $T=T^*_{\rm TC}$, then increases with J to $T\sim T^*_{\rm GD}$ and approaches $T=T^*_{\rm antiTC}$ in the anti-TCM sector.

in the inset). Three curves for $N=50$ (black), 200 (blue), and 800 (red) show that if N is increased, then r becomes closer to the universal value $r_{\rm GD}$ at the critical point $g_c/2$. In Fig. 4(c) we demonstrate a behavior of r along the critical line (see red cut in the inset). It grows from one universal value $r_{\rm TC}$ to another $r_{\rm GD}$ when J is increased from 0 to $g_c/2$. Slopes of the curves near $J=0$ increase with N. This means that the TCM and crossover sectors, determined by $J\sim\Delta$, become more narrow, because of $\Delta\propto N^{-1/2}$, and the curves approach the asymptotical value of $r_{\rm GD}$. A dependence of the Fano factor ratio $F/\mathcal{Q}$ along the critical line is shown in Fig. 5 for $N=50$ and $\beta\omega=\beta\epsilon=10$. It changes from one universal ratio $F_{\rm TC}/\mathcal{Q}$ to another $F_{\rm GD}/\mathcal{Q}$, shown as dashed blue lines. Interestingly, that dependence on J is not monotonous in the TCM sector. The gray area located at $J=\Delta$ stands for the crossover region.

In a calculation of squeezing through (42) we approximate the integrand by leading order terms for large $z\gg 1$ as $(1+\frac{I_1(z)}{I_0(z)})\approx 2$ and $(1-\frac{I_1(z)}{I_0(z)})\approx\frac{1}{2z}$. As follows from physical grounds there is no squeezing of an electric component of the photon field (squeezing along x). The leading contribution $\delta x\approx\sqrt{\langle\Phi\rangle_{\rm GD}}$ is independent on couplings for any position in the critical line $g+J=g_c$. A dependence on J appears in higher-order correction:

$$\delta x_{\rm GD}=\sqrt{\langle\Phi\rangle_{\rm GD}}\left(1-\frac{\Gamma(5/4)\omega\sqrt{\epsilon T}}{4\Gamma(3/4)\sqrt{N}gJ}\right). \tag{69}$$

The constraint $J\gg\Delta$ prevents a divergency of the correction for small J. At the TCM-to-GDM crossover, where $J\sim\Delta$, the result (69) matches with that obtained for TCM (55). For magnetic field squeezing (p direction) we find that the result is totally different from that in the TCM case:

$$\delta p_{\rm GD}=\frac{1}{2\sqrt{\beta\omega\eta_1}}=\left[\frac{T\epsilon}{8gJ}\right]^{1/2}, \tag{70}$$

namely, the temperature scaling changes from $\delta p_{\rm TC}\propto T^{1/4}$ to $\delta p_{\rm GD}\propto T^{1/2}$. It is important that δp is independent on γ in our limit of $\eta_1\gg\sqrt{\gamma}$. It is reflected in the absence of N in (70), in contrast to $\delta x_{\rm GD}\sim N^{1/4}$. It follows from (70) that the photon condensate is squeezed in p direction, i.e., $\delta p_{\rm GD}<1/2$, when $J>J_{\rm sq}$ and the threshold coupling is

$$J_{\rm sq}=\frac{\sqrt{\epsilon/\omega}}{2}T. \tag{71}$$

Thus, the GDM sector of the critical region has both nonsqueezed and squeezed phases of the photon condensate. An inversion of (71) provides a temperature scale

$$T_{\rm sq}=2J\sqrt{\frac{\omega}{\epsilon}} \tag{72}$$

below which $T<T_{\rm sq}$, a nonzero antiresonant interaction J, results in the squeezing. Note that according to (70), the maximally possible squeezing

$$\delta p_{\rm max}=\sqrt{\frac{T}{2\omega}} \tag{73}$$

appears at the symmetric point of $g=J=g_c/2$ [it is illustrated in Fig. 2(b) for a non-Goldstone potential].

Results for δp are presented in Fig. 6 where the vertical axis is an antiresonant interaction $0<J<g_c$ which determines a position on the critical region (red cut in the inset), and the horizontal axis is the temperature. Here the red cut covers the entire critical region, from TCM to anti-TCM sectors. Dashed curves are determined by relations $J=\Delta(T)$ and

$J = g_c - \Delta(T)$, they indicate positions of crossovers into the GDM sector. Blue lines are determined by relations $J = J_{\rm sq}(T)$ and $J = g_c - J_{\rm sq}(T)$, they are boundaries between squeezed and nonsqueezed condensates.

The last remark in this section concerns a correlation between dynamics of the condensate's magnitude and phase. We analyze it via the ratio α of squeezing δp and a corresponding mean-field-like factorized form:

$$\alpha = \frac{\sqrt{\langle \Phi \sin^2\varphi\rangle}}{\sqrt{\langle\Phi\rangle_{\rm GD}}\sqrt{\langle\sin^2\varphi\rangle_{\rm GD}}}, \tag{74}$$

If fluctuations of Φ and φ are decoupled from each other, then $\alpha = 1$. Correlations between of them lead to a decrease of α. The squeezing and $\langle\Phi\rangle$ which enter the expression for α were found above; in a calculation of phase fluctuations $\langle\sin^2\varphi\rangle$ we use a lower cutoff at $\phi \sim \eta_1^{-1}$ in the numerator of (42) and obtain

$$\langle\sin^2\varphi\rangle_{\rm GD} = \frac{(\gamma/\eta_1^2)^{1/4}}{4\Gamma(5/4)}. \tag{75}$$

Hence, the result for squeezed phase where $g \sim J$ is

$$\alpha \sim \left[\frac{\gamma}{\eta_1^2}\right]^{1/8} \sim \left[\frac{T}{N\epsilon}\right]^{1/8}. \tag{76}$$

The ratio is vanishing in a large N limit as $\alpha \propto N^{-1/8}$, however, the decay is rather slow. This means that a correlation between fluctuations of the phase and magnitude in the squeezed condensate becomes significant at large N. The vanishing α means that these fluctuations cannot be decoupled by a mean field.

B. Minimal temperature

We are back to the issue on the applicability of our effective theory for ψ_0 and derive here the respective minimal temperature scale T^*. At this point we give the exact definition for the photon number which involves the occupation number δn of all nonzero modes

$$\langle\hat a^\dagger\hat a\rangle_\beta = \langle\Phi\rangle + \delta n - \frac{1}{2}, \quad \delta n = \sum_{n\neq 0}\langle\bar\psi_n\psi_n\rangle. \tag{77}$$

The term $-1/2$ is due to commutation relations and is not important here. The central assumption of this work is that the leading contributions in the thermodynamic averages (37) are given by $\langle\Phi\rangle$. This means that

$$\delta n \ll \langle\Phi\rangle \tag{78}$$

providing a criterion on the smallest scale T^*. As shown above, the critical scaling of photon number remains invariant as $\langle\Phi\rangle \sim \mathcal{Q}$ in GDM, anti-TCM, TCM, and the crossover regimes. Let us analyze δn for these cases. To do that we perform a Gaussian integration with the action for nonzero $S_{\rm fl}[\bar\psi_{n\neq0};\psi_{n\neq0}]$. The result for δn at arbitrary ϵ and ω is cumbersome, however, for $\epsilon = \omega$ the following compact form is obtained for critical line $J = \omega - g$:

$$\delta n = \frac{(g+\omega)\coth\frac{\sqrt{g\omega}}{T}}{8\sqrt{g\omega}} + \frac{\omega - g}{24T} - \frac{T}{8}\left(\frac{1}{g}+\frac{1}{\omega}\right). \tag{79}$$

We focus on the case $\omega = \epsilon$ which is rather representative and allows one to find character values of T^* and its scaling with N. In contrast to leading order term $\langle\Phi\rangle$ proportional to $\mathcal{Q}$, temperature scaling of δn is sensitive to the position in the critical region. There are three limits of interest (hereafter $g_c = \omega$ and, as usual, $T \ll \omega$). The first one is given by RWA, where $J \ll \Delta$ and $g \approx g_c$. The correction and minimal temperature that follow from (78) and (79) read as

$$\delta n_{\rm TC} = \frac{1}{4} + O(T/\omega), \quad T^*_{\rm TC} = \frac{\omega}{N}. \tag{80}$$

At this point we reproduce the result of Ref. [27] on the applicability of the $S[\Phi,\varphi]$,

$$\omega \gg T \gg T^*_{\rm TC}. \tag{81}$$

In the GDM regime, the leading part in δn grows with J approaching ω as

$$\delta n_{\rm GD}(J) = \frac{1}{8}\sqrt{\frac{1}{1-J/\omega}}, \tag{82}$$

where $\omega - J \gg \Delta$. The minimal temperature also grows inverse proportional to J,

$$T^*_{\rm GD}(J) = \frac{\omega^2}{N(\omega - J)}. \tag{83}$$

A strikingly different result for the minimal temperature is found for the anti-TCM domain, where $\omega - J \sim \Delta$. In this case the leading part in δn is given by

$$\delta n_{\rm antiTC} = \frac{\omega}{24T}. \tag{84}$$

This provides the distinct scaling law for N:

$$T^*_{\rm antiTC} = \frac{\omega}{N^{1/3}}. \tag{85}$$

Thus we obtain $T^*_{\rm antiTC} \gg T^*_{\rm TC}$. It means that fluctuations above the condensate in anti-TCM are stronger than that in TCM. The difference in the scaling laws is a manifestation of that fact that these models are not dual to each other.

Numerical solution $\delta n = \mathcal{Q}$ gives a typical dependence of T^* on J. This solution is presented in Fig. 6 as the edge of the gray sector, where T^* increases with J according to the above analysis.

C. Zero-temperature limit for anti-Tavis-Cummings and Tavis-Cummings models

It is of interest to analyze in more detail zero-temperature properties of the system under consideration. Both TCM and anti-TCM limits are exactly solvable using Bethe ansatz even if inhomogeneous broadening is present in the system. Let us first consider the TCM regime. As it was already mentioned above, in this limit the excitation number is a good quantum number, since its operator commutes with the Hamiltonian. Hence, there exist sectors with different excitation numbers $N_{\rm ex}$ or with different excitation densities $\rho = N_{\rm ex}/N$, provided the thermodynamical limit $N \to \infty$ is considered. The leading in $1/N$ contribution to the ground state energy density at

given ρ is [26]

$$E_{\rm gr}(\rho)/N = \frac{1}{2}(\varepsilon - \sqrt{(\varepsilon-\lambda)^2+\xi^2}) + \lambda\left(\rho - \frac{1}{2}\right) + \frac{\xi^2}{4}(\omega - \lambda), \quad (86)$$

where both parameters ξ and λ are determined by conditions $\partial E_{\rm gr}(\rho)/\partial\xi = 0$ and $\partial E_{\rm gr}(\rho)/\partial\lambda = 0$. The ground state energy $E_{\rm gr}(\rho)$ is an extensive quantity. We stress that all other contributions to the energy are negligible in the limit $N \to \infty$, i.e., nonextensive, but they can be evaluated using the approach of Ref. [26]. At fixed ρ, parameters ξ and λ also determine energies of excited dressed states (TCM Hamiltonian eigenstates) given by $\sqrt{(\varepsilon-\lambda)^2+\xi^2}$. In this sense, ξ and λ are similar to the gap and chemical potential, respectively, while the mean-field treatment turns out to be exact in the thermodynamical limit due to a specific structure of the interaction term of the Hamiltonian (all-to-all interaction). Note that the mean density of photons is expressed through ξ as $\xi^2/2g^2$.

The global ground state of the system is given by the minimum of $E_{\rm gr}(\rho)$ as a function of ρ. It is easy to find from the above two equations that, at small enough g, this global minimum corresponds to the normal phase with $\rho = \xi = 0$. This result agrees with the perturbation theory around the noninteracting limit $g = 0$. The normal phase becomes unstable [$dE_{\rm gr}(\rho)/d\rho = 0$ at $\rho = 0$] at the critical coupling $g = g_c$ where second-order phase transition emerges. It is accompanied by the appearance of both nonzero excitation and photon densities given by ρ and $\xi^2/2g^2$, respectively.

Now we discuss the anti-TCM limit. Mathematically, it can be mapped on the TCM regime by considering another vacuum state with all qubits excited. The Hamiltonian acting on this polarized vacuum acquires an additional contribution $\varepsilon N/2$, while the excitation energies of qubits are transformed as $\varepsilon \to -\varepsilon$ and $\hat\sigma_j^+ \to \hat\sigma_j^-, \hat\sigma_j^- \to \hat\sigma_j^+$. Under such a mapping, the Bethe ansatz can be applied as well. We also should keep in mind that the normal state now corresponds to $\rho = 1$ in terms of excitations of the new vacuum state. By performing the same analysis as in the case of TCM, we find that the normal state with zero photon density becomes unstable towards a superradiant phase with nonzero photon density at the same interaction constant $J = g_c$ and the transition is also of second order. This is again in agreement with the path integral treatment.

In the view of the duality between TCM and anti-TCM, the latter result may seem as rather expectable, but we would like to stress that, by its structure, the antiresonant interaction term is quite different from the resonant one and, therefore, normal states must differ in TCM and anti-TCM limits. Indeed, the resonant term does not change an excitation number and therefore the normal phase contains exactly zero excitations. In contrast, an antiresonant term does change an excitation number and hence photons should be present even in the normal state, as follows from the perturbation theory near $g = 0$ limit. However, photon density vanishes in the thermodynamical limit, while photon number does not (this is also readily revealed using the perturbation theory). From this viewpoint, the similarity of TCM and anti-TCM is not obvious and it emerges in the thermodynamical limit only, while finite-N regimes must be different. The difference between anti-TCM and TCM can be also linked to the fact that anti-TCM is mapped on TCM with negative qubit excitation energies and physically the duality is not absolute since normal states correspond to different values of ρ. It is evident from the above considerations that finite-size corrections (in powers of $1/N$) to TCM and anti-TCM regimes differ. This latter conclusion is justified by the results derived with the use of the path integral formalism.

IV. DISCUSSION

Let us now discuss a connection of our results to that known from some other works on superradiant QPT. As was shown in Refs. [28,29], symmetric Dicke model reveals signatures of quantum chaos above the superradiant QPT if N is finite. It was shown through quasiclassical equations of motion and also through a change of the eigenvalues statistics from Poissonian, in the normal phase, to a Wigner one, above the QPT. The repulsion of levels in GDM with $g \neq J$ and an interpretation of that as quantum chaos was discussed earlier, in particular, in Ref. [42]. In that work authors demonstrated a variety of nonregular levels statistics for different g/J ratios, however, a connection with the superradiant transition was not discussed. Leaving the issue on levels statistics near the critical line $g + J = g_c$ beyond the scope of the consideration, we provided a description of the macroscopic photon condensate properties in this work implying that microscopic dynamics can be strongly chaotic. Our results on universal fluctuations and field squeezing, collected in Table I, give an alternative view on ergodic dynamics of GDM. In our approach we analyzed the non-Goldstone functional that depends on two variables, the magnitude and phase of the photon condensate. We showed that a coupling between fluctuations of these variables can be reduced to an effective dissipative action (35) for the magnitude only. (This quantity is proportional to the condensed photons amount). The functional has different asymptotical behavior depending on g-to-J ratio at the critical region of normal-to-superradiant phase transition.

Rather remarkable, a structure of the functional along $g + J = g_c$ is such that scalings of photon number and its fluctuations remains unchanged as $\langle\hat a^\dagger\hat a\rangle \sim \langle\langle\hat a^\dagger\hat a\hat a^\dagger\hat a\rangle\rangle^{1/2} \sim \mathcal{Q}$ with the scaling function $\mathcal{Q} = \sqrt{NT\epsilon/\omega^2}$. However, a sensitivity to antiresonant coupling appears in their relative values and the squeezing of magnetic filed component. The phase diagram, illustrating these sectors with different universal behaviors inside the critical region, is shown in Fig. 3. As follows from this effective theory, relative fluctuations of condensed photons can take two universal values at the critical region: $r_{\rm TC} = \frac{\pi}{2} - 1$ and $r_{\rm GD} = 4\frac{\Gamma^2(5/4)}{\Gamma^2(3/4)} - 1$, corresponding to TCM and GDM regimes, respectively. Character dependencies of relative fluctuations are depicted in Figs. 4(a) and 4(b) for these two limits. The effective action derived allows us to describe a smooth crossover between these two regimes. A similar crossover is found for the opposite anti-TCM limit as well. The domain of coupling J, where antiresonant terms in the Hamiltonian are irrelevant and the condensate behaves accordingly to finite T TCM, is limited from above as $J \ll \Delta$

TABLE I. Results for universal fluctuations, squeezing, and minimal temperature.

Regime	Relative fluctuations, r	Fano factor ratio, $F/\mathcal{Q}$	Coordinate squeezing, δx	Momentum squeezing, δp	Minimal temperature, T^*
Tavis-Cummings	$\frac{\pi}{2}-1$	$\frac{\sqrt{\pi}}{2}-\frac{1}{\sqrt{\pi}}$	$\frac{1}{\sqrt{2}\pi^{1/4}}[\frac{NT\epsilon}{\omega^2}]^{1/4}$	$\frac{1}{\sqrt{2}\pi^{1/4}}[\frac{NT\epsilon}{\omega^2}]^{1/4}$	$\frac{\omega}{N}$
Generalized Dicke	$4\frac{\Gamma^2(5/4)}{\Gamma^2(3/4)}-1$	$\frac{4\Gamma^2(5/4)-\Gamma^2(3/4)}{4\Gamma(5/4)\Gamma(3/4)}$	$\sqrt{\frac{\Gamma(3/4)}{4\Gamma(5/4)}}[\frac{NT\epsilon}{\omega^2}]^{1/4}$	$[\frac{T\epsilon}{8gJ}]^{1/2}$	$\frac{\omega^2}{N(\omega-J)}$
Anti-Tavis-Cummings	$\frac{\pi}{2}-1$	$\frac{\sqrt{\pi}}{2}-\frac{1}{\sqrt{\pi}}$	$\frac{1}{\sqrt{2}\pi^{1/4}}[\frac{NT\epsilon}{\omega^2}]^{1/4}$	$\frac{1}{\sqrt{2}\pi^{1/4}}[\frac{NT\epsilon}{\omega^2}]^{1/4}$	$\frac{\omega}{N^{1/3}}$

where the character energy scale is $\Delta=\sqrt{\omega T/N}$. In Fig. 4(c) we showed how the relative fluctuations r evolve from $r_{\rm TC}$ to $r_{\rm GD}$ when one moves along the critical region and crosses $J=\Delta$.

The Fano factor found is much greater than unity at the critical region indicating for a photon bunching effect or, in other words, for a positive photon-photon correlation. Ratios $F/\mathcal{Q}$ were found to be universal constants, again, in TCM and GDM sectors of phase diagram (their values are presented in Table I). The crossover from one universal value $F_{\rm TC}/\mathcal{Q}$ to another $F_{\rm GD}/\mathcal{Q}$ is shown in Fig. 5. The Fano factor increases by a number for $J\gtrsim\Delta$; it stands for an increase of photon-photon correlations due to the antiresonant term in the Hamiltonian and growing entanglement of eigenfunctions.

An important result is that momentum squeezing of the superradiant condensate is sensitive to the antiresonant interaction. In $U(1)$ limit of $J=0$ there is no squeezing and $\delta x=\delta p\sim\mathcal{Q}^{1/2}$. A nonzero J results in a momentum squeezing $\delta p<\delta x$. We find that it has two different temperature scalings in TCM and in GDM sectors as $\delta p_{\rm TC}\propto T^{1/4}$ and $\delta p_{\rm GD}\propto T^{1/2}$, respectively. These asymptotics are shown as dashed lines in Fig. 7 for the $\delta p(T)$ plot. An alternative representation for δp is shown in the T-J phase diagram in Fig. 6. Here the critical region reveals a squeezing of the photon condensate for antiresonant coupling $J>J_{\rm sq}=T\sqrt{\epsilon/(4\omega)}$ (blue region). Interestingly, interaction strength $J_{\rm sq}$ scales linear with T and does not depend on N.

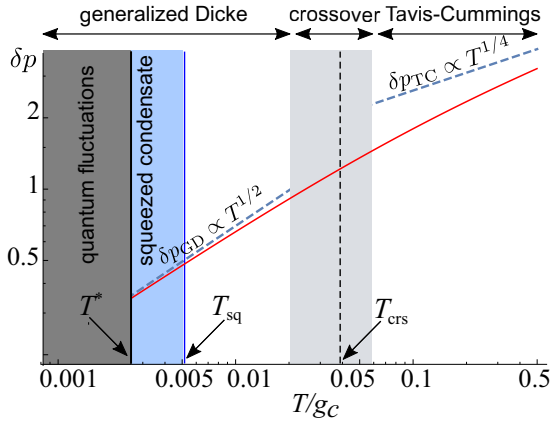

FIG. 7. The logarithmic dependence of squeezing $\ln\delta p$ as a function of $\ln T$ (red curve) and the hierarchy of temperature scales $T_{\rm crs}$, $T_{\rm sq}$, and T^* (vertical dashed blue and solid black lines). Universal behaviors for different T: TCM regime ($T>T_{\rm crs}$), TCM-to-GDM crossover ($T\sim T_{\rm crs}$, gray sector), GDM regime ($T<T_{\rm crs}$). Dashes lines: Different temperature scalings of squeezing in TCM and GDM regimes. GDM sector is subdivided into three parts: nonsqueezed condensate ($T_{\rm sq}<T<T_{\rm crs}$), squeezed condensate ($T^*<T<T_{\rm sq}$, light blue sector), and quantum fluctuational dominated regime ($T<T^*$, dark gray sector). Parameters $J=0.01g_c$, $g=0.99g_c$, $N=100$, $\epsilon=15\omega$, and $g_c=\sqrt{\omega\epsilon}\approx 3.87298\omega$.

We also show positions of character temperature domains in Fig. 7. One can see that the decrease of the temperature down to TCM-to-GDM crossover $T\sim T_{\rm crs}=NJ^2/\omega$ (light gray sector) shows a change in the scaling of δp. In the crossover regime the effect of antiresonant interaction terms becomes relevant. The universal fluctuations also change here from $r_{\rm TC}$ to $r_{\rm GD}$. Further decrease of the temperature below $T<T_{\rm sq}=2J\sqrt{\frac{\omega}{\epsilon}}$ shows the entrance into a squeezed phase of the condensate where $\delta p<1/2$ (light blue sector). This corresponds to an effect of the condensate's phase fixation. Cooling the system down to T^*, the entrance into a quantum fluctuational dominated regime occurs (dark gray sector). The hierarchy of energy scales in the critical region is $g_c\gg\{T,J_{\rm sq}\}\gg\{\Delta,T^*\}$.

The minimal temperature T^*, which determines our effective theory as $\omega\gg T\gg T^*$, corresponds to a change of the character of the phase transition: it is suggested that for $T\lesssim T^*$ normal-to-superradiant fluctuational transition changes to zero-temperature QPT. There is a decrease of thermal fluctuations in the condensate mode in comparison to quantum fluctuations encoded by a nonzero Matsubara mode. Hence, the effective theory allows us to approach QPT parametrically close for large N.

As follows from vanishing $\Delta\sim T^{1/2}$ at zero temperature, the critical region shrinks to the line. Scaling behavior changes in this case as follows. In our finite-T situation, the photon number scaling is $\propto N^{1/2}$. As shown in [31] for a symmetric model at $T=0$, photon number scales distinctly as $\propto N^{1/3}$ near the critical point. This solution was obtained via Holstein-Primakoff bosonization and applies to the normal phase below QPT. As we have already mentioned, the matching between these finite- and zero-temperature behaviors is a nontrivial issue. Similar change in finite- and zero-temperature physics was found also for the Lipkin-Meshkov-Glick finite-N model at the critical point [43].

The relation between T^* and J is shown in the phase diagram in Fig. 6 as an edge curve of the gray sector. It increases from $T^*_{\rm TC}\sim\omega/N$ in TCM limit with $J=0$ to $T^*_{\rm antiTC}\sim\omega/N^{1/3}$ in anti-TCM limit when J approaches g_c. The difference in the exponent (N^{-1} vs $N^{-1/3}$) is explained by different symmetries of the respective Hamiltonians. According to the above, for arbitrary small T large N exists such that Hilbert space dimension of a respective $\hat{H}$ compensates exponentially small Gibbs weights in the density matrix $e^{-\beta\hat{H}}$. (As a consequence, this results in a macroscopic occupation number in the condensate with finite-size fluctuations). It is supposed

to be $N \gg \omega/T$ for TCM sector in Fig. 6 and a more strict one, $N \gg (\omega/T)^3$, for the opposite sector of anti-TCM. These conditions determine a lower number of two-level systems in the ensemble when the dynamics is similar to that in the thermodynamic limit.

V. SUMMARY

In this work we investigated an effect of anisotropic interaction between a single-mode cavity and a two-level system ensemble on fluctuational properties of a photon condensate near the superradiant phase transition. Addressing the equilibrium field theory for a generalized Dicke model, we focused on a situation of simultaneously finite temperature and size of the ensemble. This regime was found to be more complex than the well-studied quantum phase transition at zero temperature [20,28–31,38] or thermodynamic limit at an infinite ensemble's size [23–26,36,37]. We showed that an increase of the antiresonant coupling changes one critical behavior, corresponding to the Tavis-Cummings or anti-Tavis-Cummings $U(1)$ models, to another one, corresponding to the generalized Dicke $\mathbb{Z}_2$ model. This transition between two fluctuational behaviors reveals a change in temperature scaling laws for squeezing parameters. The antiresonant interaction strength, above which the condensate becomes strongly squeezed, was determined. We also found explicit expressions for other universal parameters which characterize fluctuations; they do not depend on the temperature and the ensemble's size. This is, in particular, a Fano factor representing photon bunching in the condensate. The presented study, which demonstrates a richness of the critical behavior, is expected to be relevant for the understanding of many-body physics of cavity quantum electrodynamics.

The averaging with a finite temperature density matrix used as a theoretical tool in our findings assumes that the system is open. In contrast to virtual photons in a ground state at zero temperature, the condensate's photons in our finite-temperature situation can be measured [44]. This can be done by the methods employed for driven-dissipative condensate [2] where the superradiant QPT was demonstrated. Generally, nonequilibrium conditions result in a change of universality class of the dynamics. Nonetheless, open quantum systems near the critical point are known to behave effectively as equilibrium with a certain effective temperature and obey low-frequency fluctuation-dissipation relations [18,45,46].

It is suggested that our findings might be accessible in state-of-the-art realizations of strongly coupled light-matter systems [44] such as quantum metamaterials and simulators based on cold atoms, superconducting qubits, nitrogen-vacancy centers, and semiconductor based heterostructures. A possible route can be probing of the Fano factor through the counting of photon numbers over long times. They are accessible through intensity (second-order) correlation functions measurements [47] or transmission of incoherent drive [48] realized in a photon blockade effect. This allows one to identify the position of the critical region of the superradiant phase transition. Then, extracting the relative fluctuations values with the use of the counting data, one obtains information on the type of universal behavior and the respective symmetry of the interaction. Our predictions on universal fluctuations and squeezing of the photon condensate, in principle, can be measured by the dispersive readout techniques.

ACKNOWLEDGMENTS

We thank Arkady M. Satanin, Igor S. Burmistrov, and Julien Vidal for fruitful discussions. The work reported in Secs. II A–II E and Secs. III A 1–III A 3 was funded by RFBR according to the research Project No. 19-32-80014. The work reported in Secs. III B and III C was financed by the Russian Science Foundation under Grant No. 16-12-00095. Yu.E.L. acknowledges support from RFBR Project No. 20-02-00410. W.V.P. acknowledges support from RFBR Project No. 19-02-00421. D.S.S. acknowledges the funding by RFBR according to research Projects No. 20-37-70028 and No. 20-52-12034.

[1] R. H. Dicke, Phys. Rev. **93**, 99 (1954).
[2] K. Baumann, C. Guerlin, F. Brennecke, and T. Esslinger, Nature (London) **464**, 1301 EP (2010).
[3] A. Safavi-Naini, R. J. Lewis-Swan, J. G. Bohnet, M. Gärttner, K. A. Gilmore, J. E. Jordan, J. Cohn, J. K. Freericks, A. M. Rey, and J. J. Bollinger, Phys. Rev. Lett. **121**, 040503 (2018).
[4] P. Macha, G. Oelsner, J.-M. Reiner, M. Marthaler, S. André, G. Schön, U. Hübner, H.-G. Meyer, E. Il'ichev, and A. V. Ustinov, Nat. Commun. **5**, 5146 (2014).
[5] K. Kakuyanagi, Y. Matsuzaki, C. Déprez, H. Toida, K. Semba, H. Yamaguchi, W. J. Munro, and S. Saito, Phys. Rev. Lett. **117**, 210503 (2016).
[6] K. V. Shulga, P. Yang, G. P. Fedorov, M. V. Fistul, M. Weides, and A. V. Ustinov, JETP Lett. **105**, 47 (2017).
[7] W. Zhang, W. Huang, M. E. Gershenson, and M. T. Bell, Phys. Rev. Appl. **8**, 051001 (2017).
[8] S. J. Srinivasan, A. J. Hoffman, J. M. Gambetta, and A. A. Houck, Phys. Rev. Lett. **106**, 083601 (2011).
[9] A. J. Hoffman, S. J. Srinivasan, J. M. Gambetta, and A. A. Houck, Phys. Rev. B **84**, 184515 (2011).
[10] Y. Chen, C. Neill, P. Roushan, N. Leung, M. Fang, R. Barends, J. Kelly, B. Campbell, Z. Chen, B. Chiaro *et al.*, Phys. Rev. Lett. **113**, 220502 (2014).
[11] S. Zeytinoğlu, M. Pechal, S. Berger, A. A. Abdumalikov Jr, A. Wallraff, and S. Filipp, Phys. Rev. A **91**, 043846 (2015).
[12] P. Forn-Díaz, J. Lisenfeld, D. Marcos, J. J. García-Ripoll, E. Solano, C. J. P. M. Harmans, and J. E. Mooij, Phys. Rev. Lett. **105**, 237001 (2010).
[13] S. J. Bosman, M. F. Gely, V. Singh, D. Bothner, A. Castellanos-Gomez, and G. A. Steele, Phys. Rev. B **95**, 224515 (2017).
[14] C. K. Andersen and A. Blais, New J. Phys. **19**, 023022 (2017).
[15] J. Braumüller, M. Marthaler, A. Schneider, A. Stehli, H. Rotzinger, M. Weides, and A. V. Ustinov, Nat. Commun. **8**, 779 (2017).
[16] S. Putz, D. O. Krimer, R. Amsuess, A. Valookaran, T. Noebauer, J. Schmiedmayer, S. Rotter, and J. Majer, Nat. Phys. **10**, 720 (2014).

[17] A. Angerer, K. Streltsov, T. Astner, S. Putz, H. Sumiya, S. Onoda, J. Isoya, W. J. Munro, K. Nemoto, J. Schmiedmayer *et al.*, Nat. Phys. **14**, 1168 (2018).
[18] P. Kirton, M. M. Roses, J. Keeling, and E. G. Dalla Torre, Adv. Quantum Technol. **2**, 1800043 (2019).
[19] G. Wang, R. Xiao, H. Z. Shen, C. Sun, and K. Xue, Sci. Rep. **9**, 4569 (2019).
[20] A. Baksic and C. Ciuti, Phys. Rev. Lett. **112**, 173601 (2014).
[21] Z. H. Wang, Q. Zheng, X. Wang, and Y. Li, Sci. Rep. **6**, 22347 (2016).
[22] Q.-T. Xie, S. Cui, J.-P. Cao, L. Amico, and H. Fan, Phys. Rev. X **4**, 021046 (2014).
[23] V. N. Popov and S. Fedotov, Sov. Phys. JETP **67**, 535 (1988).
[24] P. R. Eastham and P. B. Littlewood, Phys. Rev. B **64**, 235101 (2001).
[25] P. R. Eastham and P. B. Littlewood, Phys. Rev. B **73**, 085306 (2006).
[26] W. Pogosov, D. Shapiro, L. Bork, and A. Onishchenko, Nucl. Phys. B **919**, 218 (2017).
[27] D. S. Shapiro, A. N. Rubtsov, S. V. Remizov, W. V. Pogosov, and Y. E. Lozovik, Phys. Rev. A **99**, 063821 (2019).
[28] C. Emary and T. Brandes, Phys. Rev. Lett. **90**, 044101 (2003).
[29] C. Emary and T. Brandes, Phys. Rev. E **67**, 066203 (2003).
[30] A. Altland and F. Haake, Phys. Rev. Lett. **108**, 073601 (2012).
[31] J. Vidal and S. Dusuel, Europhys. Lett. **74**, 817 (2006).
[32] Y. Alavirad and A. Lavasani, Phys. Rev. A **99**, 043602 (2019).
[33] R. J. Lewis-Swan, A. Safavi-Naini, J. J. Bollinger, and A. M. Rey, Nat. Commun. **10**, 1581 (2019).
[34] J. Chávez-Carlos, B. López-del-Carpio, M. A. Bastarrachea-Magnani, P. Stránský, S. Lerma-Hernández, L. F. Santos, and J. G. Hirsch, Phys. Rev. Lett. **122**, 024101 (2019).
[35] L. Bakemeier, A. Alvermann, and H. Fehske, Phys. Rev. A **85**, 043821 (2012).
[36] M. A. Alcalde and B. Pimentel, Physica A **390**, 3385 (2011).
[37] M. A. Alcalde, A. L. L. de Lemos, and N. F. Svaiter, J. Phys. A: Math. Theor. **40**, 11961 (2007).
[38] M. Liu, S. Chesi, Z.-J. Ying, X. Chen, H.-G. Luo, and H.-Q. Lin, Phys. Rev. Lett. **119**, 220601 (2017).
[39] J. Martin, Proc. R. Soc. London Ser. A **251**, 536 (1959).
[40] A. M. Tsvelik, *Quantum Field Theory in Condensed Matter Physics* (Cambridge University Press, Cambridge, 2007).
[41] P. Schad, Y. Makhlin, B. Narozhny, G. Schön, and A. Shnirman, Ann. Phys. **361**, 401 (2015).
[42] C. Lewenkopf, M. Nemes, V. Marvulle, M. Pato, and W. Wreszinski, Phys. Lett. A **155**, 113 (1991).
[43] J. Wilms, J. Vidal, F. Verstraete, and S. Dusuel, J. Stat. Mech.: Theory Exp. (2012) P01023.
[44] A. Frisk Kockum, A. Miranowicz, S. De Liberato, S. Savasta, and F. Nori, Nat. Rev. Phys. **1**, 19 (2019).
[45] L. M. Sieberer, S. D. Huber, E. Altman, and S. Diehl, Phys. Rev. Lett. **110**, 195301 (2013).
[46] E. G. D. Torre, S. Diehl, M. D. Lukin, S. Sachdev, and P. Strack, Phys. Rev. A **87**, 023831 (2013).
[47] C. Lang, D. Bozyigit, C. Eichler, L. Steffen, J. M. Fink, A. A. Abdumalikov, M. Baur, S. Filipp, M. P. da Silva, A. Blais *et al.*, Phys. Rev. Lett. **106**, 243601 (2011).
[48] A. J. Hoffman, S. J. Srinivasan, S. Schmidt, L. Spietz, J. Aumentado, H. E. Türeci, and A. A. Houck, Phys. Rev. Lett. **107**, 053602 (2011).